# Macro- and microlensing

Stefan Palenta (Jena)

*This contribution wants to point out similarities and differences between optical and gravitational lenses. Extensive use of Fermat's principle is made. Then the two different manifestations of gravitation lensing are discussed: macrolensing and its imaging properties for radially symmetric lenses, as well as microlensing and its applications.*

## Introduction: What does "lensing" mean?

From traditional optics, we are familiar with diverging and converging lenses. They impose to each light ray a time delay which is proportional to the length of its way through the glass. In terms of the thin lens approximation the lens can be described as an infinitesimally thin sheet causing time delays which depend on the light ray's point of transition through that sheet. For a converging lens, this delay is maximal on the optical axis and decreases radially outward, for the diverging lens the time delay is minimal in the center and increases radially outward. According to Fermat's principle, a light ray always chooses a path of minimal time. In the presence of a lens, this means that a light ray does not connect two points on opposite sides of the lens via a straight line, but via a refracted line where the point of transition through the lens is shifted to smaller time delays (figure 1). This viewpoint serves as an alternative explanation for the inward refraction of the converging lens and the outward refraction of the diverging lens and will help dealing with gravitational lenses.

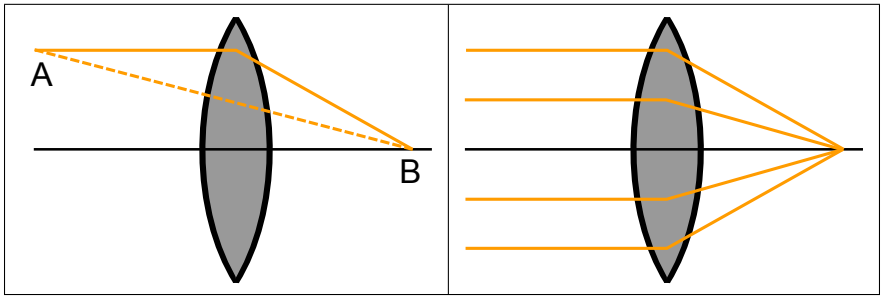


Figure 1: *left:* the light ray from A to B takes a refracted path according to Fermats principle; *right:* focusing of a converging lens.

Now we take a closer look at the converging lens by considering a bunch of light rays parallel to the optical axis of the lens. As already said, the imposed time delay decreases radially outward. The bending angle of a single ray, which is proportional to the gradient of the time delay, increases with its distance $d$ from the optical axis so that the whole bunch is focused into a single point (figure 1).

Gravitational lenses can be interrelated with optical lenses via the refractive index approximation: For weak gravitational fields, the field's action on light rays can be described by an effective index of refraction, calculated from the Newtonian potential $|\Phi|$ as $n = 1 + \frac{2}{c^2}|\Phi|$. The thin lens approximation in optics corresponds to the thin screen approximation for gravitational lenses. Again, the lens is described as an infinitesimally small sheet causing time delays which depend on the light ray's point of transition through the sheet. As in optics, this is valid for small deviation angles.

The simplest example for such a gravitational lens is a point mass with a potential $|\Phi| \sim \frac{1}{r}$ (figure 2). In the thin screen approximation, it causes a similarly looking time delay profile when plotted over the distance $d$ from the optical axis. We now see that for the gravitational point

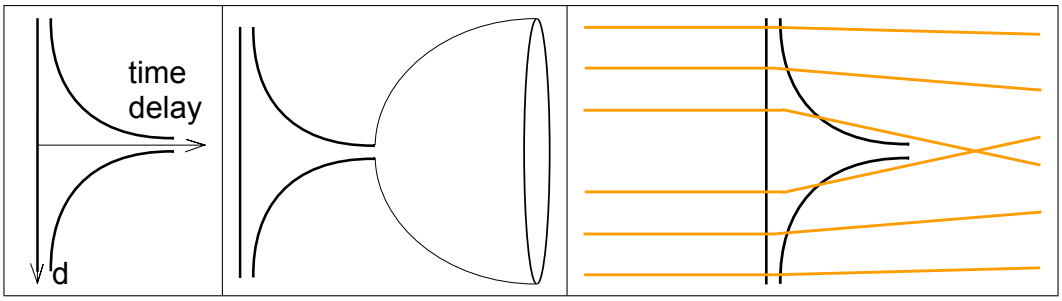


Figure 2: *left:* time delay profile of a gravitational point mass lens; *middle:* wine glass to simulate a point mass lens; *right:* non-focusing of a point mass lens.

mass lens, the bending angle for light rays initially parallel to the optical axis decreases with $d$. In consequence there is no focusing of a bunch of light rays, and so the term gravitational "lens" means just a thing that disturbs light rays. Another obvious thing now is how to simulate a gravitational point mass lens with an optical one: we simply have to take the foot of a wine glass.

## Distinction between macro- and microlensing

Having clarified that gravitational lenses have in general no focusing properties, we now remember some properties of the images generated by a gravitational point mass lens. In the picture on the right [1], the source is located on the sky at the point $S$. But with the lens present in point $M$ deflecting the light, there arise two different images $I_-$ and $I_+$ which are seen by an observer instead of the source $S$. The first one is located inside the circle around $M$ with the Einstein radius $\Theta_E$ and the second one lies outside this circle. The separation between the images is about the double of the Einstein radius. This enables us to distinguish between the phenomenon of macrolensing, where those two images can be resolved, and microlensing where this is not the case. Both cases shall be introduced by an example:

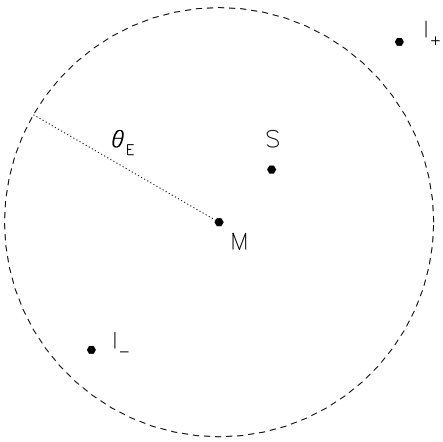


**Example 1: Macrolensing of two galaxies:**

| | |
|---|---|
| Distance to the source: | $D_S = 1Gpc$ |
| Distance to the lens: | $D_L = 0{,}25Gpc$ |
| Mass of the lens: | $D_S = 1Gpc$ |
| $\rightarrow$ Einstein radius: | $\Theta_E = 1{,}6''$ |

$\Rightarrow$The single images are resolveable, typical images like stretched galaxies and Einstein rings occur.

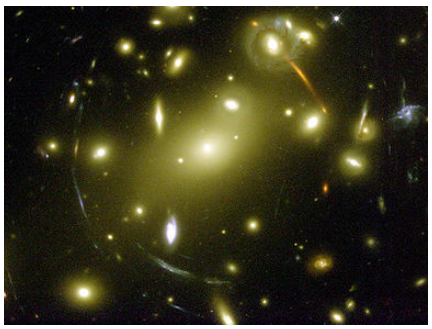

Figure 3: Macrolensing of the Galaxy Cluster Abell 2218 [4].

**Example 2: Microlensing of a galactic halo object:**

| | |
|---|---|
| Distance to the source: | $D_S = 53kpc$ (in the LMC) |
| Distance to the lens: | $D_L = 8kpc$ (in galactic halo) |
| Mass of the lens: | $M_L = 1M_\odot$ |
| $\rightarrow$ Einstein radius: | $\Theta_E = 0{,}001''$ |

$\Rightarrow$ The single images are not resolveable, only an apparent increase in the source's brightness occurs.

## Macrolensing of galaxies

So far we always dealt with gravitational lensing by point mass lenses. In this section we will derive a generalization to extended matter distributions as lenses. We start with radially symmetric lenses and then briefly discuss deviations from radial symmetry.

Within the thin screen approximation, it is allowed and useful to project the matter distribution of an extended lens onto the lens plane. For now this projection should be radially symmetric, as it is approximately the case for a globular cluster or a spiral galaxy viewed from the top. There are a few models for radially symmetric matter distributions as described in figure 4.

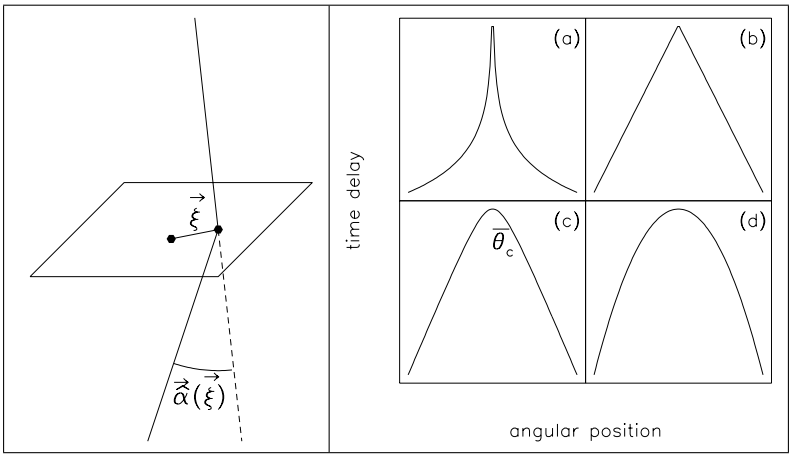


Figure 4: *left:* thin screen approximation: the effect of the lens is described by the lens plane where the light ray changes its direction instantaneously [1]; *right:* common potential models for radial lenses: the already known point mass (a), the so called singular isothermal sphere (b) with a central density going to infinity, the softened isothermal sphere (c) with a homogeneous core of radius $\theta_c$ and the constant density sheet (d). Remarkably, the last configuration is the only gravitational lens with focusing properties [1].

In the refractive index approximation, a light ray travelling from the source around the lens to the observer can be delayed for two reasons:

- the geometrical time delay $t_{geom}$ due to the additional way around the lens
- the gravitational time delay $t_{grav}$ directly caused by the lens via its index of refraction

These time delays can be just added up to a total time delay $t_{total}$ within the thin screen approximation, which is illustrated in figure 5. According to Fermat's principle, the real light rays take paths of extremal time (This is in fact a very clarifying example for the use of Fermat's principle concerning local (i.e. possibly multiple) extrema (and not just minima)).

This discussion yields in general three different extremal paths for light travelling from the source to the observer, two outer local minima and an inner local maximum of time delay. Therefore the observer can see three different images of the source. The outer two were already introduced as the images $I_-$ and $I_+$ of a point mass, the third one happens to be infinitely faint for singular central mass densities.

Furthermore, the chosen treatment of gravitational lensing via time delays enables us to discuss different angular distances between the source and the lens. This distance is expressed

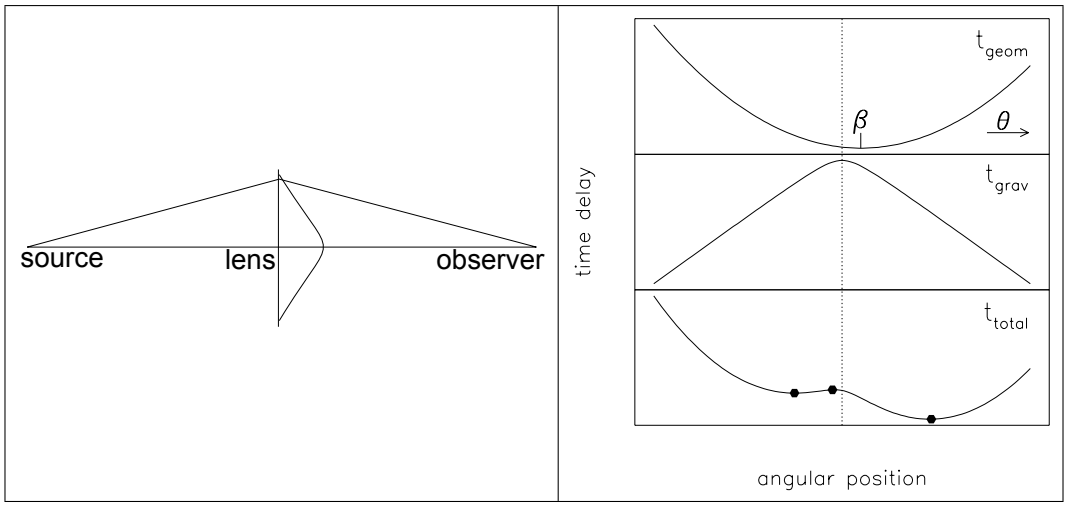


Figure 5: *left:* setup for a light ray passing the lens; *right:* geometrical time delay $t_{geom}$, gravitational time delay $t_{grav}$ and their sum $t_{total}$ plotted over the radial distance in the lens plane [1].

by the relative shift between the midpoints of the geometrical and the gravitational time delay in figure 5. In consequence, the shape of the total time delay changes when that distance varies.

For the discussion we regard the lens as fixed and think of the source moving behind it (figure 6). We start from the collinear case where source, lens and observer lie on one line in space. The total time delay is symmetric and due to the radial symmetry, both outer images degenerate to an Einstein ring. Now the angular separation between source and lens grows and the total time delay gets deformed. Finally, there is a special configuration where two of the images meet and vanish, which is easy to understand as annihilation of a local minimum and maximum in the total time delay.

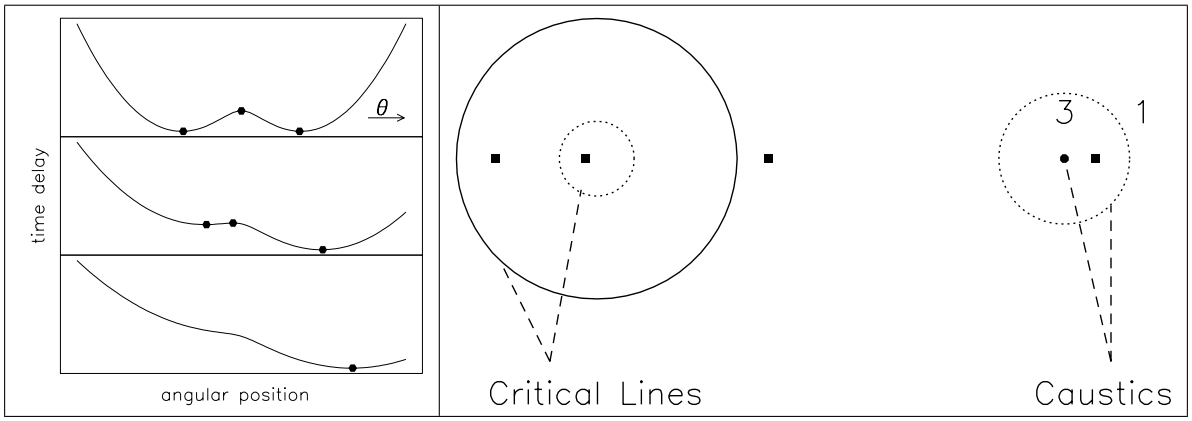


Figure 6: *left:* total time delay $t_{total}$ for different positions of the source with three and one extremum, respectively [1]; *right:* critical lines and caustics of a radially symmetric lens [1].

The points in the lens plane where the images meet and vanish or degenerate are called critical lines (figure 6). A radial symmetric lens has its Einstein ring as a degenerated critical line. Inside of it lies another circular critical line, where images could meet and vanish. The positions of the source in the source plane corresponding to the critical lines are called caustics. A central pointlike caustic belongs to the Einstein ring, a circular caustic belongs to the other critical line.

By now we have established the vocabulary to qualitatively address lenses which deviate from radial symmetry. The simplest of such deviations is the generalization to elliptic mass distributions, which could arise from projections of tilted galaxies.

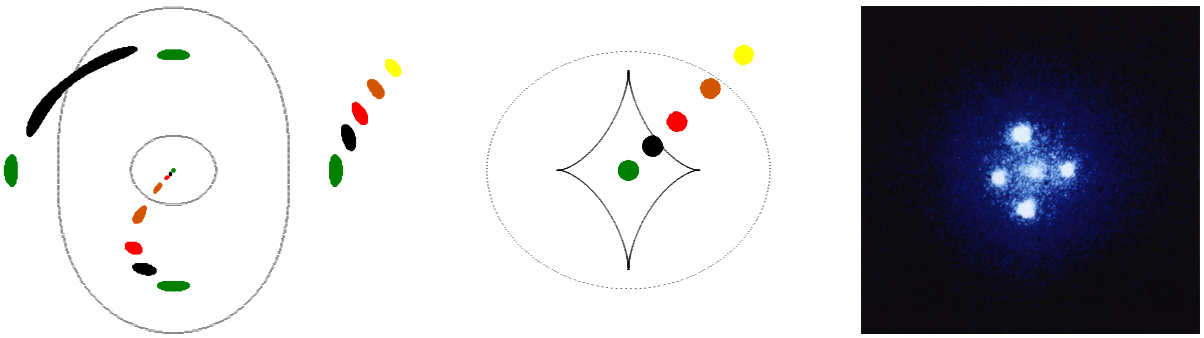

Figure 7: *left:* critical lines and caustics of an elliptic lens [1]; *right:* "Einstein cross" Q2237+030 in Pegasus [4].

On the transition to an elliptic lens both critical lines as well as the outer caustic become ellipses. However, the inner pointlike caustic extends to a diamond shaped figure with 4 sharp points as shown in figure 7. The images outside both caustics and between inner and outer caustic are similar to the radially symmetric case (yellow, orange, red). But a source inside the inner caustic generates two additional images (black, green), which form an Einstein cross (green) rather than an Einstein ring in the collinear case. The Einstein cross Q2237+030 in Pegasus is a very famous observation of macrolensing.

## Microlensing of point masses

In the second section we defined microlensing as those setups of gravitational lensing, where the single images cannot be resolved and the only effect is an apparent increase in the source's brightness. For simplicity we constrain ourselves to point mass lenses again in this section.

The lens, as seen from the source, covers only a little solid angle. Therefore the lens plane can be considered uniformly illuminated by the source. Hence the brightness measured by the observer is proportional to the area in the lens plane where the images are located. The enhancing factor $\mu$ due to the microlensing effect is thus the fraction of the image size and the source area in the lens plane. The corresponding surface elements are illustrated by the picture on the right [1]. With the source position $\beta$ the enhancing factor can be calculated as

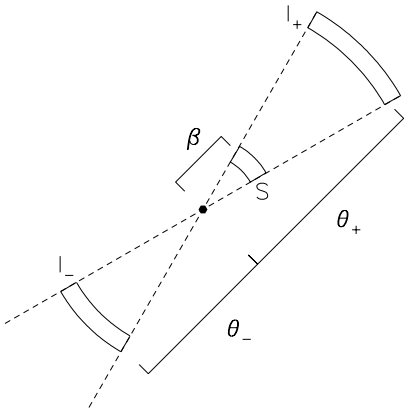


$$\mu = \frac{\Delta\Omega}{(\Delta\Omega)_0} = \left|\frac{\sin\Theta d\Theta d\phi}{\sin\beta d\beta d\phi}\right| \approx \left|\frac{\Theta}{\beta}\frac{d\Theta}{d\beta}\right|$$

The angular radii of the two Images $I_-$ and $I_+$ are given by

$$\Theta_{+,-} = \frac{1}{2}\Theta_E\left(u \pm \sqrt{4+u^2}\right) \quad \text{with} \quad u = \frac{\beta}{\Theta_E}$$

So we get the single enhancement factors

$$\mu_{+,-} = \frac{\left(\sqrt{4+u^2} \pm u\right)^2}{4u\sqrt{4+u^2}}$$

The total enhancement is therefore

$$\mu_{tot} = \mu_+ + \mu_- = \frac{2+u^2}{u\sqrt{4+u^2}} > 1$$

For the limiting case $\beta \gg \Theta_E$ of large angular separation between source and lens we get

$$u = \frac{\beta}{\Theta_E} \gg 1 \quad \Rightarrow \quad \mu_{tot} \approx 1$$

The case $\beta = \Theta_E$ delivers

$$u = 1 \quad \Rightarrow \quad \mu_{tot} = \frac{3}{\sqrt{5}} \approx 1,34$$

as a typical value for the enhancement factor.

A microlensing event now denominates the process where source and lens approximate each other up to a minimal angular distance and depart again. This corresponds to a typical development of the enhancement factor over time. The corresponding brightness curves are shown in figure 8. They are characterised by their strict time symmetry and monochromacy (i.e. independence of colour). The maximum of enhancement depends on the minimal angular distance.

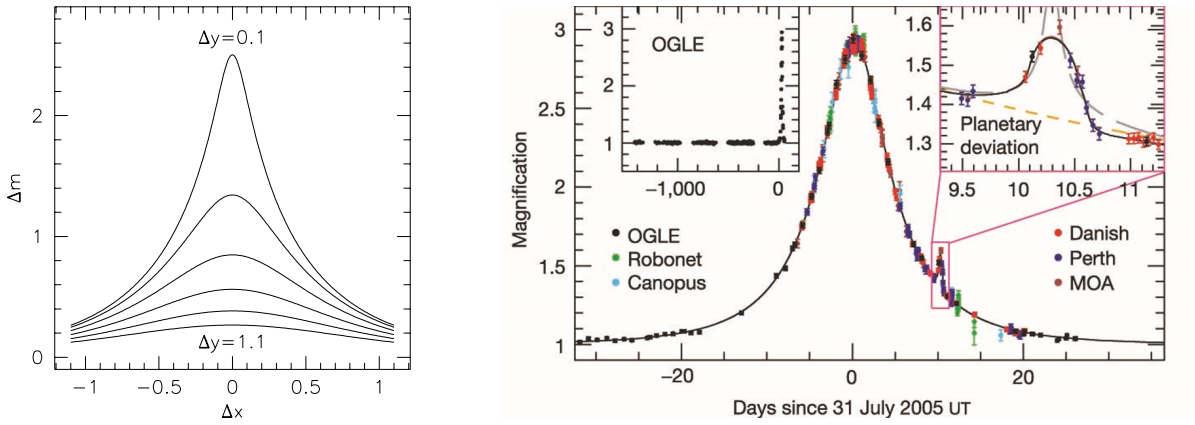


Figure 8: *left:* development of the magnification $\mu_{tot}$ for different minimal angular distances [1]; *right:* accumulated data from a microlensing event with the discovery of a planetary companion [5].

The careful observation of microlensing events is a modern method to discover exoplanets. The frequency of microlensing events is also used to determine the density of compact dark objects in the halo of our galaxy. These investigations showed that this density is to low to explain the dark matter effects.

## References

[1] Narayan R., Bartelmann M.: *Lectures on gravitational lensing*; in: Formation of Structure in the Universe, Proceedings of the 1995 Jerusalem Winter School; Cambridge University Press.

[2] Refsdal S.: *The gravitational lens effect*; Monthly Notices of the Royal Astronomical Society 128(1964) 295.

[3] Boonserm P. et al: *Effective refractive index tensor for weak-field gravity*; Class. Quantum Grav. 22(2005) 1905.

[4] Picture from NASA's space telescope Hubble.

[5] Beaulieu J.-P. et al.: *Discovery of a Cool Planet of 5.5 Earth Masses Through Gravitational Microlensing* Nature 439(2006) 437.